Mott–Peierls phase in deuterated copper-DCNQI systems: a comprehensive study of longitudinal and transverse conductivity and ageing effects

2003 J. Phys.: Condens. Matter 15 7351

(http://iopscience.iop.org/0953-8984/15/43/017)

INSTITUTE OF PHYSICS PUBLISHING JOURNAL OF PHYSICS: CONDENSED MATTER

J. Phys.: Condens. Matter **15** (2003) 7351–7364 PII: S0953-8984(03)65539-6

Mott–Peierls phase in deuterated copper-DCNQI systems: a comprehensive study of longitudinal and transverse conductivity and ageing effects

Marko Pinterić[1,2,3], Tomislav Vuletić[1], Martin Lončarić[1], Konstantin Petukhov[2], Boris Gorshunov[2,4], Jost Ulrich von Schütz[2], Silvia Tomić[1] and Martin Dressel[2]

[1] Institut za Fiziku, PO Box 304, HR-10001 Zagreb, Croatia
[2] Physikalisches Institut, Universität Stuttgart, D-70550 Stuttgart, Germany

E-mail: stomic@ifs.hr

Received 1 July 2003, in final form 8 September 2003
Published 17 October 2003
Online at stacks.iop.org/JPhysCM/15/7351

Abstract

Transport and low-frequency optical reflection measurements (180–380 GHz) are reported for the quasi-three-dimensional conducting alloy $Cu[(2,5(CH_3)_2\text{–DCNQI})_{0.70}(2,5(CD_3)_2\text{–DCNQI})_{0.30}]_2$ between room temperature and 35 K. The optical properties of the system are strongly anisotropic. It is metallic down to 60 K where a Mott–Peierls phase transition occurs. While the transverse conductivity remains practically unchanged, the longitudinal conductivity abruptly drops at the phase transition. Comparing our latest results with previous dc data and measurements of the microwave conductivity also reported here, we find indications of an ageing effect in these samples.

1. Introduction

Considerable efforts have been devoted to explore the novel class of charge-transfer salts $Cu(2,5R_1R_2\text{–DCNQI})_2$ (where DCNQI stands for dicyanoquinonediimine and $R_1, R_2 = CH_3$, CH_3O, Cl, Br, I etc) because of its rich phase diagram, in which physical properties can be easily controlled by varying external (pressure, magnetic field) and internal (isotope substitution, doping) parameters [1–3]. A theoretically and experimentally interesting case of the above described property happens for the $R_1 = R_2 = CH_3$ salt, where either the application of a small pressure or gradual deuteration changes the ground state of the material. Since deuteration is an easily controllable experimental parameter, this enables a precise study of the phase diagram. The undeuterated system $Cu(2,5(CH_3)_2\text{–DCNQI})_2$

[3] Permanent address: Faculty of Civil Engineering, University of Maribor, SLO-2000 Maribor, Slovenia.
[4] Permanent address: General Physics Institute, Russian Academy of Sciences, Moscow, Russia.

(abbreviated as h_8) shows fully metallic behaviour throughout the whole temperature range, while the fully deuterated system Cu(1,4D_2; 2,5$(CD_3)_2$–DCNQI)$_2$ (abbreviated as d_8) shows one sharp entrance into the insulating state at about 80 K. Most interestingly, a range of partially deuterated systems, as well as the alloys between undeuterated and deuterated systems like Cu[(2,5$(CH_3)_2$–DCNQI)$_{0.70}$(2,5$(CD_3)_2$–DCNQI)$_{0.30}$]$_2$ (abbreviated as h_8/d_6 70%:30%), show both a sharp transition in the insulating state and a reentrance back to the metallic state at low temperatures.

This unusual behaviour is ascribed to the unique property that the copper electrons of the highest occupied 3d orbital interact with DCNQI electrons of the highest occupied pπ orbital [4]. In addition to one-dimensional (1D) pπ bands, associated with DCNQI chains and observed in DCNQI crystals containing no copper, the three-dimensional (3D) Fermi surface appears since DCNQI chains are mutually interconnected *via* tetrahedrally coordinated Cu ions. The density of states at the Fermi level is enhanced by the mixing of pπ and 3d orbitals, which is consistent with a high room temperature (RT) longitudinal (along the *c*-axis) conductivity of the order of 1000 Ω^{-1} cm^{-1}. Further, it turns out that the valence of Cu is crucial for the observed metal-to-insulator and insulator-to-metal phase transitions. Its valence in the metallic state is somewhat smaller than +4/3 and differs slightly among samples with and without a low-temperature insulating state [4]. The decrease of the temperature or the increase of the internal or external pressure results in the distortion of the coordination tetrahedron, which induces an extra charge transfer to DCNQI molecules. Eventually this structural change locks the Cu valence to exactly +4/3 with static charge ordering at the copper sites (. . . $Cu^{2+}Cu^{1+}Cu^{1+}$ . . .). This is accompanied by the phase transition into the insulating state with the formation of the charge-density wave (CDW) in DCNQI chains along the *c*-axis. Indeed, the CDW was confirmed by the appearance of the three-fold superstructure with strong intensity of the observed satellite spots [5, 6]. CDW dynamics was studied by low-frequency dielectric spectroscopy and dc electric-field-dependent transport measurements [7, 8]. However, it should be noted that although the dc conductivity measurements show an abrupt change in resistivity, the concomitant existence of a huge hysteresis, as well as the results obtained by dielectric [7] and ESR measurements [9], suggest that the insulating CDW and metallic phases also coexist near the phase transition. This phase transition, coined as the Mott–Peierls phase transition, is explained as a result of the Peierls transition with three-fold lattice distortion in the presence of strongly correlated Cu d-states [10]. In other words, in addition to electron–phonon interaction, strong electron–electron correlations and a 3D coupling are shown to be necessary ingredients, which have to be taken into account to describe the observed phase diagram properly.

Despite extensive research efforts, not much is known about the temperature dependence, as well as the mechanism of the transverse conductivity $\sigma_\perp$. In the Bechgaard salts $(TMTSF)_2X$, which represent typical quasi-1D organic materials with only one band (simple quasi-1D Fermi surface), the conductivity amounts to $\sigma_a = 500\,\Omega^{-1}$ cm^{-1} for the longitudinal direction and $\sigma_b = 20\ \Omega^{-1}$ cm^{-1} and $\sigma_c = 0.03\ \Omega^{-1}$ cm^{-1} for the two transverse directions [11]. While σ_a and σ_b have their origin in the band-like conduction, σ_c is due to the electron hopping between molecular stacks. In the copper-DCNQI salts a somewhat larger longitudinal conductivity $\sigma_\parallel$ is primarily due to the existence of the 3D band in addition to the 1D bands. The question arises if the existence of the 3D band also enhances the transverse conductivity. Tajima *et al* [12] performed optical reflection measurements on the Cu(1D; 2,5$(CD_3)_2$–DCNQI)$_2$ member of copper-DCNQI family (abbreviated as d_7). The reported results reveal a metallic behaviour both parallel and perpendicular to the chains with an anisotropy of about 3–5 in the mid-infrared range, which changes by only a small amount above the phase transition. In the insulating phase the Drude component completely disappears

in both directions. Another interesting issue concerns the effect of the phase transition on the band structure. The 3D network above the phase transition is related to the mixed valence of the copper atoms and should disappear with static charge ordering at the Cu atoms in the insulating state. Therefore the measurement of the conduction anisotropy might be very helpful in obtaining a clearer and consistent picture regarding these open issues. Finally, almost nothing is known about possible sample ageing effects and their influence on the stabilisation of the Mott–Peierls insulating state. In order to get an insight into this issue, we have performed an extensive study consisting of more than 100 cycles on about 125 single crystals of the h_8/d_6 70%:30% and of 10 cycles on 5 single crystals of the d_8 copper-DCNQI systems throughout a seven year period.

2. Experimental details and results

2.1. Synthesis procedure

Single crystals of d_8 and h_8/d_6 70%:30% were synthesized in 1995 using the electrochemical method. The copper perchlorate acetonitril complex and either $Cu(1,4D_2;2,5(CD_3)_2\text{–DCNQI})_2$ or the mixture of $Cu(2,5(CH_3)_2\text{–DCNQI})_2$ and $Cu(2,5(CD_3)_2\text{–DCNQI})_2$ were dissolved in acetonitril and put into a cell with a glass diaphragm and two platinum electrodes. A current of about 5 μA was imposed on the electrodes for about two weeks. All measurements reported in this paper were made on the single crystals taken from one batch of the d_8 material and from one batch of the h_8/d_6 70%:30% material. Thin needles in these two batches were morphologically best defined and had varying lengths from 2 to 10 mm and cross sections from 0.001 to 0.01 mm^2. The samples were kept in closed compartments in the dark for long periods between two consecutive measurements.

2.2. Dc conductivity measurements

The dc conductivity measurements were performed on nine h_8/d_6 70%:30% single crystals in 1999 and on 13 h_8/d_6 70%:30% single crystals in 1999/2000 (the end of 1999 and the beginning of 2000). They were also performed on three d_8 single crystals over about the same period of time. The RT conductivity was in the range 800–1200 Ω^{-1} cm^{-1}. The measurements were performed using the standard four contact dc technique or using the two contact method and a Keithley 617 electrometer in V–I mode. Contacts were attached along the needle either by silver paste or carbon paste diluted in hexyl-acetate solvent. This enabled us to measure the conductivity along the c-axis of the crystal, which corresponds to the longitudinal conductivity $\sigma_{\parallel}$. The upper limit of the contact resistances measured in the insulating phase was estimated to be smaller than 1% and 0.001% of the sample resistance, when the silver and carbon paste were used, respectively. The thermal treatment of the samples consisted of different cooling/warming rates and various thermal history. Typically, cooling rates were -20 K h^{-1} above liquid nitrogen temperature, and -60 K h^{-1} below.

On cooling from RT down to 100 K, the longitudinal conductivity increases by about one order of magnitude [9]. Below that temperature the conductivity saturates or even changes to a slight decrease. A typical behaviour observed for the conductivity *versus* temperature for h_8/d_6 70%:30% below 100 K is shown in figure 1. It represents one possible full thermal cycle, consisting of two half-cycles. The first half-cycle is obtained by cooling the sample from 80 K to as low as 4.2 K, depending on the cycle, whereas the second is obtained by warming the sample back to 80 K. It should also be noted that the conductivity at 60 K is about the same as the RT conductivity due to the sample cracks that occurred between 80 and 120 K, which decrease the conductivity by one order of magnitude. In the cooling half-cycle the sample undergoes two

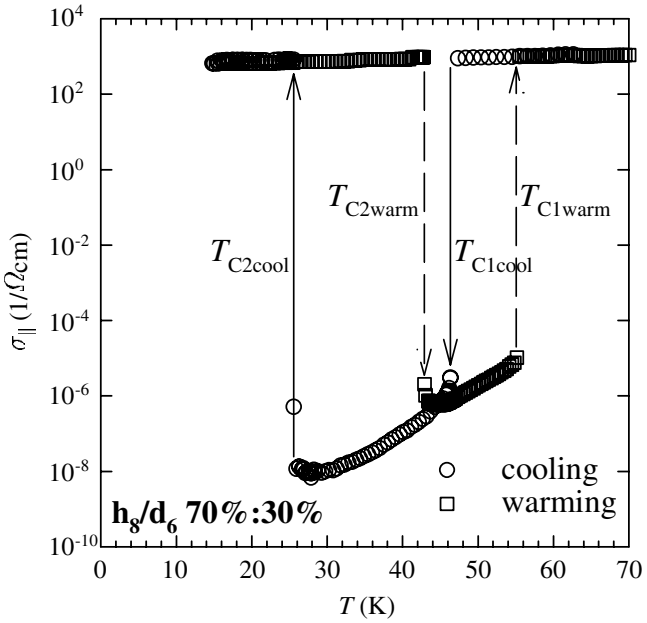

Figure 1. A typical conductivity versus temperature cycle below 100 K with two phase transitions in the cooling and in the warming half-cycle, obtained by dc conductivity measurements.

sharp phase transitions, metal-to-insulator (entry) at $T_{C1cool} = 46$ K and insulator-to-metal (re-entry) at $T_{C2cool} = 26$ K. Because of the huge hysteresis area, the entry $T_{C2warm} = 43$ K and the re-entry $T_{C1warm} = 55$ K temperatures in the warming half-cycle differ significantly from those in the cooling half-cycle. This is in full agreement with previously published results [9, 13]. It should be also noted that all four phase transition temperatures vary among different cycles by about ± 5 K. This temperature variation was obtained for the same thermal treatment conditions, that is for typical cooling rates, and appears not only among different samples but among different cycles for a particular sample as well. In order to resolve the origin of this effect, we also changed the thermal treatment of the samples; however, we were unable to find any firm correspondence between the thermal treatment and the phase transition temperature variation.

During the investigation another curious feature showed up. Samples often missed the insulating phase in the cooling half-cycle, or in the warming half-cycle, or there was no insulating phase in the whole cycle. One typical situation with two phase transitions in the cooling half-cycle and no phase transition in the warming half-cycle is shown in figure 2. The situation was further complicated by the fact that the same sample in the same thermal treatment conditions behaved differently from one cycle to another.

Extensive measurements were performed in order to resolve these anomalies. Altogether more than 100 cycles on 22 h_8/d_6 70%:30% single crystals were performed in the study, and various parameters, like cooling rate and time spent just above the highest and below the lowest phase transition temperature, were carefully controlled in order to find a memory effect pattern. Indeed we succeeded in identifying a few conditions, which successfully *suppress* the insulating phase with a high degree of certainty, in agreement with the memory effect assumption. Fast cooling rates (quenching) suppressed the insulating phase in cooling and in warming, while long times spent at the lowest temperature of the cycle in the metallic phase suppressed the insulating phase in the warming half-cycle. However, even in these 'harsh' conditions rare appearances of the insulating state were observed.

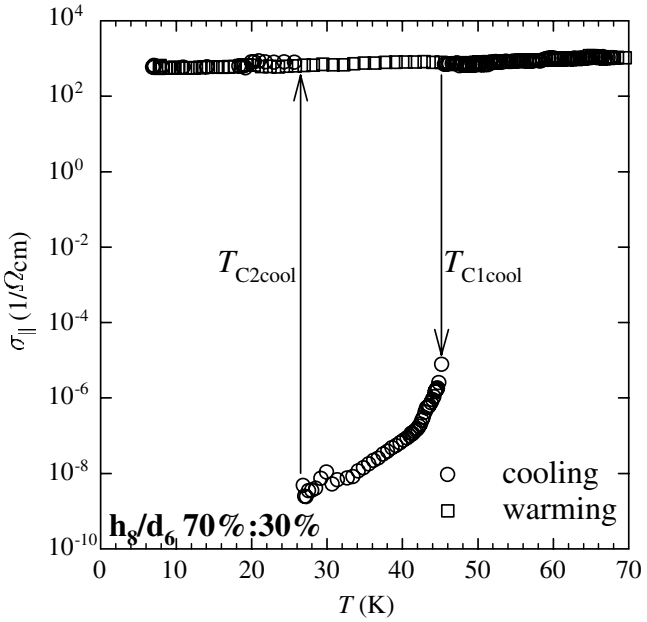

Figure 2. An instance of a conductivity versus temperature cycle below 100 K with two phase transitions in the cooling half-cycle and no phase transition in the warming half-cycle, obtained by dc conductivity measurements.

On the other hand, we did not succeed in identifying any condition that *induces* the insulating state with a high degree of certainty. We have identified 'best' conditions, which however still give a low probability of insulating states. To demonstrate our findings, we analysed the statistics of the insulating state entrances in the cooling half-cycle, but only in the 'best', well-defined slow-cooling conditions of about -60 K h^{-1}. From the 61 cycles on nine different samples in 1999 we have observed 45 entrances into the insulating state (74%). On the other hand, from the 23 cycles on 13 different samples in 1999/2000 we have observed 14 entrances into the insulating state (61%). It should be noted that most samples showed both behaviours (existence and non-existence of the insulating state) and that statistics for a particular sample were in good agreement with the overall statistics.

Finally, we would like to mention that we also performed seven cycles on three single crystals of the d_8 system, which all showed the metal-to-insulator transition. However, the number of cycles/samples is too small to allow us to make any conclusion concerning the effect observed in the h_8/d_6 70%:30% system.

2.3. Microwave cavity perturbation measurements

The microwave measurements were first performed on three h_8/d_6 70%:30% single crystals in 2002, using the conventional perturbation technique [14]. A single crystal was placed in the antinode of the electric field parallel to the electric field direction, which enabled reliable measurement of the longitudinal conductivity $\sigma_\parallel$. The centre point of the sample was mounted on the end of a quartz needle using a tiny amount of vacuum grease. Two different cavities designed for frequencies 24 and 33.5 GHz were used in the experiment. The samples were cooled typically at -20 K h^{-1} over the whole temperature range.

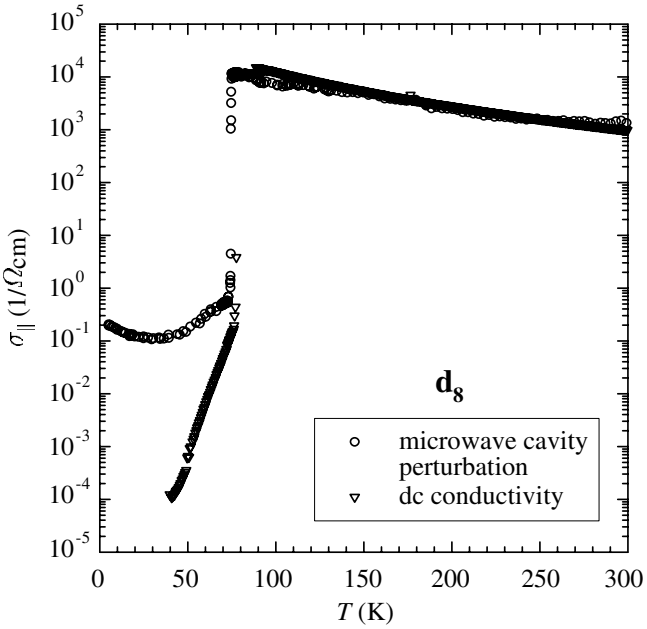

Figure 3. Longitudinal conductivity for d_8 single crystals versus temperature, obtained in cooling by dc conductivity measurements and microwave cavity perturbation measurements at 24 GHz.

No phase transition into the insulating state was seen in any of the measured samples either in cooling or in the warming half-cycle. Since there is no stress applied to the crystal in this kind of experiments, these results cannot be explained by some physical artefact. The results are, however, consistent with our dc conductivity measurements, where often the insulating state is not entered.

Two deuterated d_8 crystals were also measured at both available frequencies, 24 and 33.5 GHz. The measurements taken in cooling clearly showed the phase transition into the insulating phase at 75 K, while our dc conductivity results showed $T_C = 77$ K (see figure 3). The conductivity in the metallic phase, the phase transition temperature and the conductivity drop at the phase transition agree well with the values obtained by dc conductivity measurements. However, while dc conductivity measurements show strong conductivity activation below the phase transition temperature, microwave measurements of $\sigma_{\|}$ saturate. Similar properties were already reported for fresh h_8/d_6 70%:30% samples [15]. The authors argued that this suggests that highly conducting areas exist even in the low conducting region. Their volume part was estimated to be about 0.1%. Here, we would like to suggest another possible explanation, which assumes the existence of additional phonon or CDW modes, which influence the conductivity already at microwave frequencies by their low-frequency wing.

2.4. Submillimetre quasi-optical measurements

In order to measure the optical conductivity, both longitudinal $\sigma_{\|}$ and transverse $\sigma_{\perp}$, we performed low-frequency optical measurements in 2002. We used a coherent source quasi-optical spectrometer, which enables the measurement of different optical properties, both transmission T and reflection R, in a wide temperature range between 1.5 K and RT using a He cryostat [16].

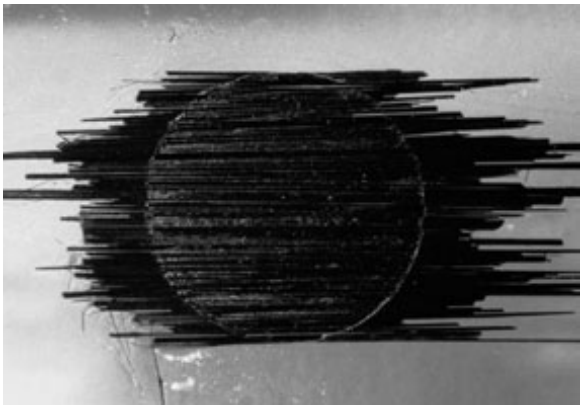

Figure 4. A photograph of the h_8/d_6 70%:30% sample mosaic. The diameter of the hole in the Mylar is 5 mm.

The requirement for reliable reflectivity results is that the sample dimensions are larger than the wavelength of the radiation. To satisfy this requirement, a mosaic of h_8/d_6 70%:30% single crystals was created, as shown in figure 4. Two holes of diameter $d = 5$ mm were made in the Mylar. After that about 100 needles were carefully aligned and fixed on both sides of the first hole using vacuum grease, while an aluminium mirror, as a reference, was mounted mechanically on the position of the second hole. The foil is tightly pressed on one side to the metallic block with a diaphragm of the 5 mm diameter; sample and reference mirror are exchanged by translation of the foil. The measurements were done in the frequency range $\nu = 180$–380 GHz and for light polarization being parallel or perpendicular to the crystal needles.

To obtain the reflectivity of the sample, both radiation intensities reflected from the sample I and the mirror I_0 are measured. Taking the temperature dependent aluminium reflectivity R_0 from literature data, one can finally obtain the sample reflectivity:

$$R = \frac{I}{I_0} R_0. \tag{1}$$

Following this procedure, the reflectivity of the sample was directly measured in the temperature range between RT and 35 K; the conductivity was subsequently extracted.

The mosaic was cooled using the cooling rates of -20 and -40 K h^{-1} above and below liquid nitrogen temperature, respectively. For temperatures above 60 K the reflectivity R for both directions is very large and does not exhibit a strong frequency dependence (see figure 5), which points to typical metallic behaviour in the limit of low ($\nu \ll \gamma$) frequencies, where γ represents the electron scattering frequency. On the basis of these considerations, in order to obtain the conductivity at zero frequency, that is, $\sigma(\nu = 0) = \sigma_0$, we can use the Hagen–Rubens expression for the frequency dependent reflectivity of a metal

$$R = 1 - 2\sqrt{\frac{4\pi\epsilon_0\nu}{\sigma_0}} \tag{2}$$

where ϵ_0 is the permittivity of vacuum. However, below 60 K, whereas the reflectivity value for the perpendicular polarisation does not change significantly, the value for the longitudinal polarisation decreases (figure 6). Nevertheless, the reflectivity is still so large that we can suppose predominantly metallic behaviour even in this temperature range. Therefore, we have

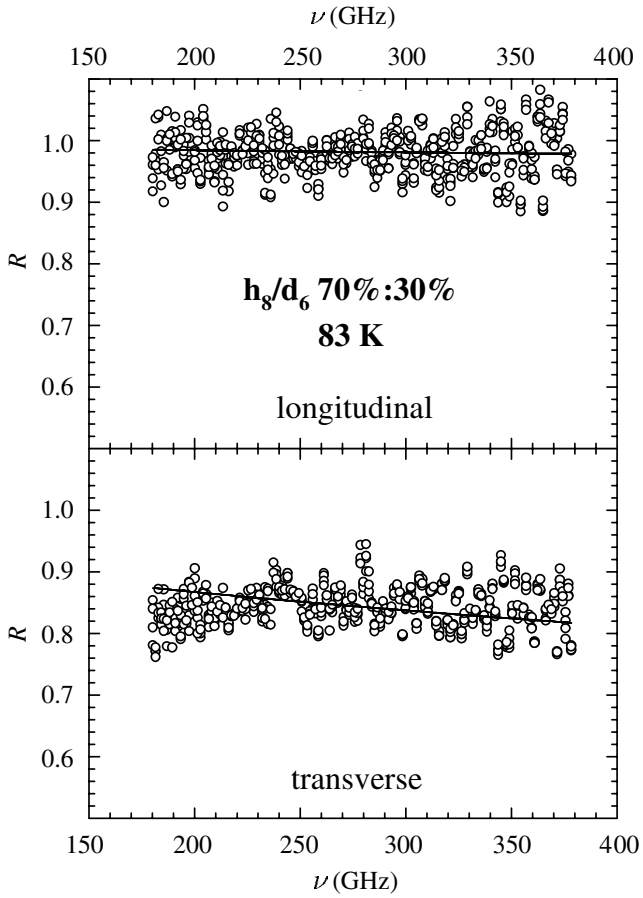

Figure 5. Reflectivity versus frequency for longitudinally and transversely polarized radiation above the phase transition range at 83 K. Full lines are fits to the Hagen–Rubens expression (see text).

used the Hagen–Rubens expression in the whole temperature range studied, but the results below 60 K should be regarded to be more qualitative than quantitative.

The results for longitudinal and transverse conductivity are shown in figure 7 for the entire temperature range. Each point corresponds to one measurement, which usually consisted of four frequency sweeps between 180 and 380 GHz, as presented in figures 5 and 6. Two points should be noted. First, the transverse conductivity is merely an average conductivity of two transverse conductivities because the transverse crystal axes a and b are, unlike the longitudinal axis c, randomly oriented. Second, in the temperature range between 40 and 80 K we tried to measure with a fast cooling rate in order to get close to the typical cooling rate of -60 K h^{-1} from dc conductivity measurements and still to obtain as many temperature points as possible. For this reason, we did not take data for the transverse conductivity in this range of temperatures. We also did not average such a large number of data points for the longitudinal conductivity, leading to much larger experimental uncertainties, as indicated by the error bars (see figure 7). As a result, an average cooling rate of -40 K h^{-1} was achieved.

The longitudinal conductivity obtained amounts to $\sigma_{\parallel} = 600\ \Omega^{-1}\ \mathrm{cm}^{-1}$ at RT and follows a metallic behaviour between RT and 60 K, which is in full accordance with previously reported

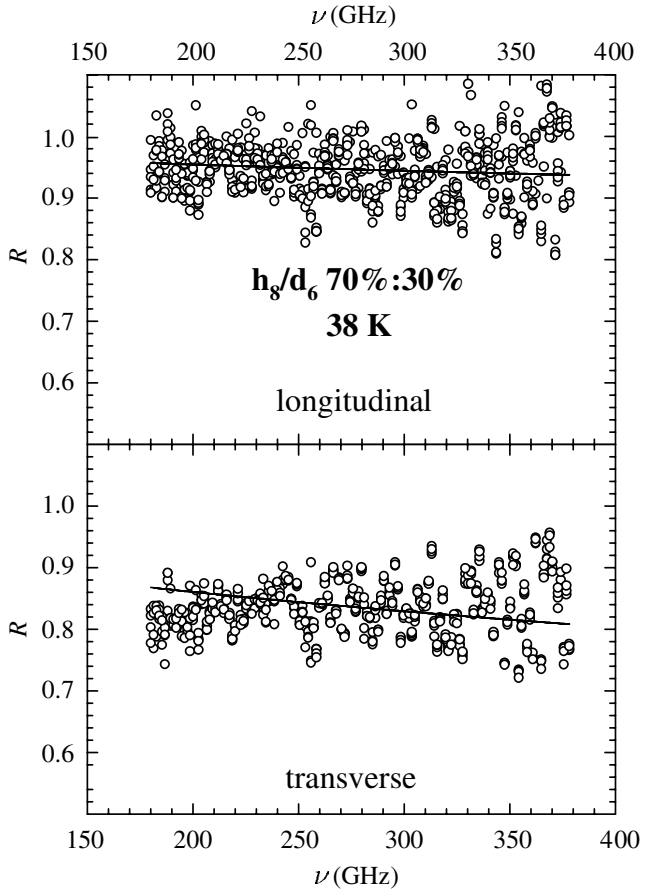

Figure 6. Reflectivity versus frequency for longitudinally and transversely polarized radiation below the phase transition range at 38 K. Full lines are fits to the Hagen–Rubens expression (see text).

results for the dc conductivity [9] and confirms that our metallic approximation for the data analysis is valid. Further, transverse conductivity amounts to $\sigma_\perp = 20\ \Omega^{-1}\ \mathrm{cm}^{-1}$ at RT, which gives an anisotropy factor of 30. The transverse conductivity also follows metallic behaviour, but this behaviour is less pronounced than in the case of the longitudinal one, so that the anisotropy factor increases to almost 10^3 at 60 K. The anisotropy values at RT and 60 K agree reasonably well with crude estimates reported previously [15]. Further, the temperature dependence of the anisotropy is in very good agreement with the one found for h_8 crystals using the cavity perturbation method [17].

The situation below 60 K, where a Mott–Peierls phase transition occurs, changes significantly. The longitudinal conductivity $\sigma_\parallel$ drops by about two orders of magnitude between 60 and 40 K. However, this decrease is much smaller than the one observed in dc conductivity measurements. Usually it is expected that a drop in conductivity at a phase transition is much larger in dc than in ac conductivity measurements, since in dc conductivity measurements one probes only the influence of free carriers, while ac conductivity measurements may be influenced by phonon and CDW modes as well. Nevertheless, taking into consideration that the reflectivity is as large as 96% and that the phase transitions were often missed in our

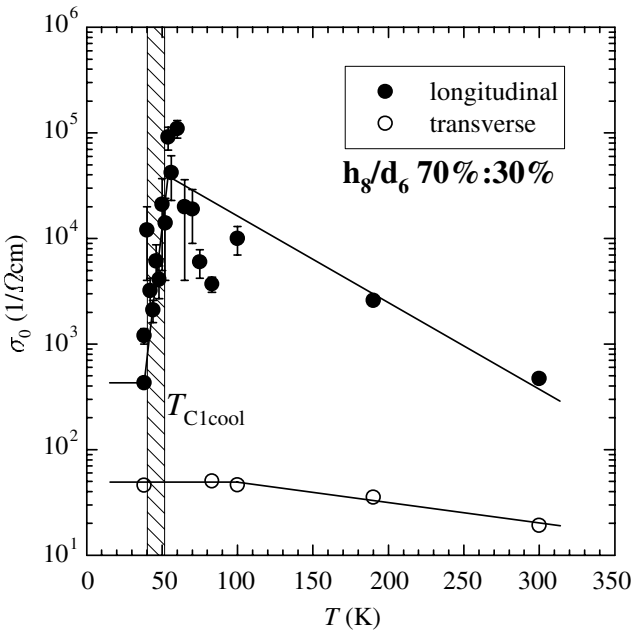

Figure 7. Longitudinal and transverse conductivity versus temperature, obtained by submillimetre quasi-optical measurements. The shaded area represents the variation of T_{C1cool} among different samples. The full lines are guides for the eye.

previous dc conductivity and microwave cavity perturbation measurements, we conclude that the smallness of the drop in submillimetre quasi-optical measurements is not solely due to phonon and CDW modes. We propose that only a small fraction of single crystals that constitute the measured mosaic (specimen) actually underwent the phase transition to an insulating state, while the conductivity of the rest of the samples remained metallic, which as a result gives predominantly metallic behaviour. It should also be noted that the quite continuous decrease of the optical conductivity, in contrast to the sharp decrease in dc conductivity measurements, is probably due to slightly different phase transition temperatures for various needles. That is, dc conductivity measurements show that this phase transition temperature varies for the same thermal treatment conditions in the range of 42 K $< T_{\mathrm{C1cool}} <$ 52 K (see section 2.2), which corresponds to the variation obtained in the submillimetre quasi-optical measurements 40 K $< T_{\mathrm{C1cool}} <$ 52 K (shaded area in figure 7).

In order to verify our suggestion that the response of the mosaic, below the Mott–Peierls phase transition, originates from two different phases we have to drop the assumption that all samples are metallic and that the Hagen–Rubens expression is valid for the whole mosaic. Instead, we can try to calculate the contribution to overall measured reflectivity coming from the metallic and from the insulating part of the mosaic. Therefore we assume that at low temperatures X is the part of the mosaic area that is insulating (R_{i}), while $1 - X$ is the part of the mosaic that is still metallic (R_{m}), giving together the reflectivity of the whole mosaic (R). That is,

$$X R_{\mathrm{i}} + (1 - X) R_{\mathrm{m}} = R. \tag{3}$$

As far as the reflectivity R_{m} of the needles (metallic part) which did not undergo the phase transition below 60 K is concerned, it should be equal to the one measured above 60 K that amounts to 0.996 and corresponds to the metallic conductivity of $\sigma_{\parallel} = 44\,000\ \Omega^{-1}\ \mathrm{cm}^{-1}$.

Further, we estimate the reflectivity R_i of the needles that entered the insulating state. According to the dc measurements, the conductivity should decrease by about *seven* orders of magnitude at the phase transition, reaching values as low as 0.0044 Ω^{-1} cm^{-1}. Thus the free electrons basically do not contribute to the reflectivity. However, considering the possibility of contributions from phonons or collective modes, we estimate R_i to be in the range $0.7 > R_i > 0.5$. The overall reflectivity of the mosaic at 35 K amounts to $R = 0.957$, which points to predominantly metallic behaviour even at this temperature. Finally, putting $R_m = 0.996$, $0.7 > R_i > 0.5$ and $R = 0.957$ in equation (3), we get $0.13 > X > 0.08$. We conclude that despite this rather crude estimate of R_i, the result of the calculation does not change much and is more or less reliable. Therefore we can safely say that about 10% of total mosaic area or approximately 10% of total needle number is in the insulating state. The estimate is reliable for longitudinal polarisation, since in this case the electric field vector of the radiation is parallel to the needles. That assures that one photon probes only one needle at a time, which is either in the metallic or the insulating state, so no averaging over different conductivity tensors (effective medium approach) is necessary.

On the other hand, the transverse conductivity $\sigma_\perp$ values above and below the phase transition do not significantly differ (figure 7). The estimate of the eventual conductivity change is within the experimental error of the experiment, which amounts to approximately 25% of the total value. Therefore this change is too small to allow us to make estimates of the insulating crystal proportion as in the case of the longitudinal conductivity.

3. Discussion

First we point out that our results for the conductivity anisotropy $\sigma_\parallel/\sigma_\perp$ agree well with those already obtained for other copper-DCNQI salts in the metallic state. While the anisotropy value at RT amounts to about 30, it steadily increases to about 10^3 just above the metal–insulator phase transition. This behaviour suggests that the 3D network, which enhances the longitudinal conductivity, strengthens as the temperature lowers. If we compare our data with results obtained for the Bechgaard salts where the average transverse conductivity is about $\sigma_\perp \approx 1\ \Omega^{-1}$ cm^{-1}, we see that the anisotropy in the material under study is much smaller, primarily due to the much larger averaged transverse conductivity. This suggests that the perpendicular conductivity might be enhanced by the 3D Fermi surface as well. On the other hand, the transverse conductivity increases at a much slower rate than the longitudinal one, excluding the previous assumption. However, polarized reflection measurements in the mid-infrared clearly indicate that the transverse conductivity is coupled to the 3D Fermi surface [12]. The Drude-like infrared absorption disappears for polarizations both parallel and perpendicular to the chains. Unfortunately, our results obtained below the phase transition do not enable us to conclude on the anisotropy in the insulating state. This is due to the facts that (a) only a certain fraction of crystals underwent the phase transition and (b) optical measurements in the insulating state may be influenced by phonon and CDW modes.

The second important result concerns the effect of the phase transition on the reflectivity of the sample. While the observed effect is huge for the longitudinal reflectivity, it is experimentally imperceivable for the transverse reflectivity. The former implies the immense drop of the longitudinal conductivity, which is well explained by the 3D network disappearance below the phase transition. On the other hand, the latter shows that the transverse conductivity remains almost unchanged in the phase transition region. This finding, as well as only a weak increase toward lower temperatures, led us to conclude that the transverse conductivity is not intimately connected with the 3D network. This seems to be in contrast to the conclusion obtained by Tajima *et al* [12] who observe a large change in the optical properties also

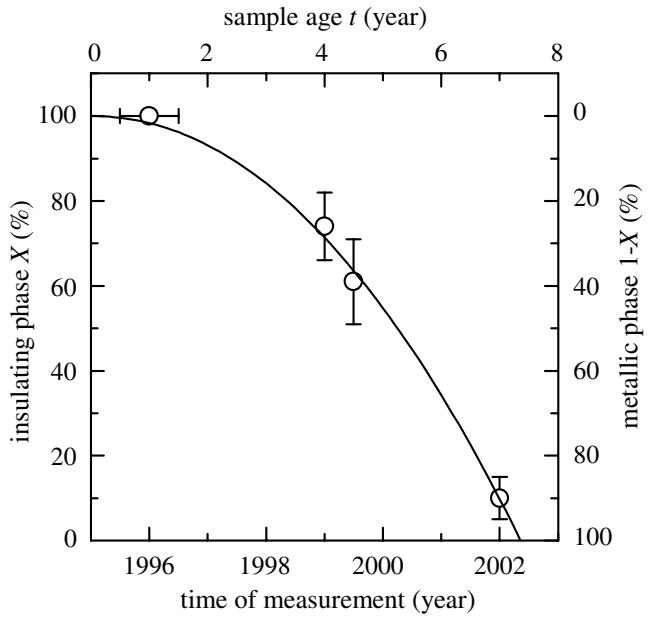

Figure 8. The percentage of metallic phase $(1 - X)$ occurrences in the cooling half-cycle for 'best', well-defined, slow-cooling conditions as a function of the sample age. The full curve is the fit to the power-law. The point with the horizontal error bar is based on the data obtained on fresh samples (see text).

perpendicular to the chains. However, compared to our experiments they probe in an energy range more than three orders of magnitude larger, with no data taken below 650 cm^{-1}. Both observations can be put in agreement if we assume incoherent transverse transport at low energies, which is not affected by the metal-to-insulator transition, while the high-energy response is changed in the same way parallel and perpendicular to the chains.

Finally, we have also established the interesting effect that some samples did not enter the insulating state. Since we performed almost 100 cycles using about 125 samples at well-defined slow-cooling conditions, we can provide reliable statistics of the insulating phase occurrence rate. We assume that one sample in submillimetre quasi-optical measurements is statistically equivalent to one cycle in dc measurements, since in the former measurements only one thermal cycle for each sample was made. Therefore, all our statistics are actually made for the cycles, almost 200 in total, of all samples studied in dc conductivity and optical measurements. Such statistics could be scaled to the age of the samples, which gives us the results shown in figure 8. Further, we note that no problem ever occurred when samples were measured shortly after synthesis. The results obtained in ESR, as well as in dc conductivity measurements, regularly gave entry and re-entry phase transitions (see for example [9]). This fact excludes the possibility that the observed ageing effect in dc conductivity measurements is due to the stress to the sample imposed by the mounting procedure. This conclusion is also supported by the finding that a particular sample, despite being under the same amount of stress, may enter the insulating phase or remain in the metallic phase. The stress can also be safely excluded as a cause of ageing in our microwave measurements, in which the sample was fixed by grease only at one point. Finally, the amount of stress was certainly larger in our optical measurements since samples were fixed by grease at two points. However, we argue

that the created stress was still too small to influence the observed results. That is, the grease was applied only at the very ends of the samples, and the samples were in this way fixed to a rather flexible Mylar. Further, despite the fact that the same amount of stress was exerted on all the samples in the mosaic, some samples did enter into the insulating phase.

We propose that the observed ageing effect might be attributed to a competition between the metallic phase and the insulating Mott–Peierls phase. In a percolation process an increase of metallic islands in the sample, which tend to connect with each other, creates highly conducting paths [18]. It is expected that the percolation behaviour is manifested by the power-law dependence. Indeed, we find a correlation between the sample age t and metallic phase proportion $1 - X$ in the form of

$$1 - X = At^{\alpha} \tag{4}$$

where A and α represent fit parameters. The power-law parameter value of $\alpha = 2.1 \pm 0.2$ (see figure 8) is in the range of standard values observed in the systems in which percolation models apply [18].

4. Conclusion

Partially and fully deuterated copper-DCNQI salts were studied using dc conductivity, microwave cavity perturbation and submillimetre quasi-optical measurements. The longitudinal conductivity shows a strong temperature dependence, as well as a huge change in the Mott–Peierls phase transition region, confirming the first-order character of the phase transition and the assumption that longitudinal conductivity is enhanced by the 3D Fermi surface. On the other hand, we have shown that the transverse conductivity follows a weak temperature dependence and does not change abruptly in the region of the phase transition, which suggests that it is not intimately connected with the 3D network. The study of crystals spanning over a period of seven years also showed a curious ageing effect in partly deuterated DCNQI salts. We show that this behaviour can be explained if the percolation behaviour connected to the coexistence of metallic and insulating islands within the sample is assumed.

Acknowledgments

We thank B Korin-Hamzić and M Prester for useful discussions. This work was partially supported by Deutsche Forschungsgemeinschaft (DFG) and the Croatian Ministry of Science and Technology.

References

[1] Werner H P, von Schütz J U, Wolf H C, Kremer R, Gehrke M, Aumüller A, Erk P and Hünig S 1988 *Solid State Commun.* **65** 809
[2] Tomić S, Jérome D, Aumüller A, Erk P, Hünig S and von Schütz J U 1988 *J. Phys. C: Solid State Phys.* **21** L203
[3] Kato R, Sawa H, Aonuma S, Tamura M, Kinoshita M and Kobayashi H 1993 *Solid State Commun.* **85** 831
[4] Kato R 2000 *Bull. Chem. Soc. Japan* **73** 515
[5] Kobayashi A, Kato R, Kobayashi H, Mori T and Inokuchi H 1987 *Solid State Commun.* **64** 45
[6] Nogami Y, Date T, Oshima K and Arimoto O 1997 *Synth. Met.* **86** 2073
[7] Pinterić M, Vuletić T, Lončarić M, Tomić S and von Schütz J U 2000 *Eur. Phys. J.* B **16** 487
[8] Vuletić T, Pinterić M, Lončarić M, Tomić S and von Schütz J U 2001 *Synth. Met.* **120** 1001
[9] Gómez D, von Schütz J U, Wolf H C and Hünig S 1996 *J. Physique* I **6** 1655
[10] Ogawa T and Suzumura Y 1996 *Phys. Rev.* B **53** 7085
[11] Korin-Hamzić B, Basletić M and Maki K 1998 *Europhys. Lett.* **43** 450

[12] Tajima H, Aonuma S, Sawa H and Kato R 1995 *J. Phys. Soc. Japan* **64** 2502
[13] Bauer D, von Schütz J U, Wolf H C, Hünig S, Sinzger K and Kremer R K 1993 *Adv. Mater.* **5** 829
[14] Donovan S, Klein O, Dressel M, Holczer K and Grüner G 1993 *Int. J. Infrared Millim. Waves* **14** 2459
[15] Predak S, Helberg H W and von Schütz J U 1995 *Acta Phys. Pol.* A **87** 791
[16] Kozlov G and Volkov A 1988 *Top. Appl. Phys.* **74** 51
[17] Burkert R, Helberg H W and von Schütz J U 1993 *Synth. Met.* **55–57** 2519
[18] Stauffer D and Aharony A 1992 *Introduction to Percolation Theory* (London: Taylor and Francis)